Eur Radiol (2006) 16: 1298–1307
DOI 10.1007/s00330-006-0184-7

MUSCULOSKELETAL

Nicolae Bolog
Daniel Nanz
Dominik Weishaupt

Muskuloskeletal MR imaging at 3.0 T: current status and future perspectives

Received: 8 December 2005
Revised: 24 January 2006
Accepted: 27 January 2006
Published online: 16 March 2006

N. Bolog · D. Nanz · D. Weishaupt (✉)
Institute of Diagnostic Radiology,
University Hospital,
Rämistrasse 100,
8091 Zurich, Switzerland
e-mail: dominik.weishaupt@usz.ch
Tel.: +41-44-2553059
Fax: +41-44-2554443

Abstract Magnetic resonance (MR) imaging has become an important diagnostic tool in evaluation of the musculoskeletal system. While most examinations are currently performed at magnetic field strengths of 1.5 T or lower, whole-body MR systems operating at 3.0 T have recently become available for clinical use. The higher field strengths promise various benefits, including increased signal-to-noise ratios, enhanced T2* contrast, increased chemical shift resolution, and most likely a better diagnostic performance in various applications. However, the changed T1, T2, and T2* relaxation times, the increased resonance-frequency differences caused by susceptibility and chemical-shift differences, and the increased absorption of radiofrequency (RF) energy by the tissues pose new challenges and/or offer new opportunities for imaging at 3.0 T compared to 1.5 T. Some of these issues have been successfully addressed only in the very recent past. This review discusses technical aspects of 3.0 T imaging as far as they have an impact on clinical routine. An overview of the current data is presented, with a focus on areas where 3.0 T promises equivalent or improved performance compared 1.5 T or lower field strengths.

Keywords MR imaging · 3 Tesla · Musculoskeletal imaging

Introduction

Magnetic resonance (MR) imaging, with its free selection of imaging planes and excellent soft-tissue contrast is widely used for the noninvasive assessment of the musculoskeletal system. The clinical impact of this diagnostic modality is highlighted by the fact that musculoskeletal imaging is the fastest growing field in MR imaging after neuro-radiological applications [1]. The goal of MR examination is a detailed assessment of the anatomical structures, an accurate evaluation of the pathological changes, and, possibly, the gathering of functional information. The ideal MR examination should provide high quality images without significant restrictions such as cost, accessibility and scanning duration. To date, clinical musculoskeletal MR imaging is commonly performed in MR systems operating at magnetic field strengths between 0.2 and 1.5 T. Although, some authors [2, 3] have shown that low-field MR imaging may be used efficiently in daily clinical practice, most musculoskeletal MR examinations are performed at magnetic field strengths of 1.0 or 1.5 T.

Recently 3.0 T MR systems have become available for clinical use. Although 3.0 T MR systems are used particularly for neuroradiological applications, several studies [4–7] have demonstrated the advantages of imaging at a higher magnetic field strength in different areas of body MR imaging. MR imaging at 3.0 T allows high spatial resolution imaging of the pelvis which may be useful in assessing gynecological tumors [4]. Promising results have also been reported for 3.0 T MR imaging in assessing diffuse lung diseases [7], and there is evidence that an increased diagnostic value of cardiac imaging may also expected from MR imaging at 3.0 T [6]. Regarding the musculoskeletal disorders several studies [8–11] have demonstrated improved imaging quality and speed in imaging of musculoskeletal disorders at 3.0 T and provided

preliminary evidence for concomitant improvement in diagnostic accuracy.

We describe here the rationale and some technical particularities of MR imaging at 3.0 T with an emphasis on tissue contrast, chemical shift, susceptibility, and specific absorption rate (SAR). We then provide an overview of the current status of musculoskeletal MR imaging at 3.0 T with a focus on the comparison between high field MR imaging (i.e., at field strengths of 2.0 T or higher) and lower magnetic field strengths (i.e., below 1.5 T). Finally, we discuss prospects of the clinical applications of 3.0 T MR systems.

Rationale for Imaging at 3.0 T

The recent development of 3.0 T whole-body MR systems has led to a special interest in musculoskeletal applications. The drive towards higher magnetic fields is based mainly on the increased MR signal and a higher signal-to-noise ratio (SNR) [8–12]. The increased SNR may enable imaging with a higher resolution and a faster acquisition of the musculoskeletal and nervous structures [13, 14]. The maximum contrast-to-noise ratios (CNRs) also depend on the magnetic-field strength. It has been shown that the CNRs between muscle and bone, between bone and cartilage, and between cartilage and fluid may all be higher at 3.0 T than at 1.5 T [8, 9]. The potential advantages have aroused anticipations of better image quality and higher diagnostic accuracy. Only a limited number of studies have until now demonstrated superior effectiveness of musculoskeletal imaging at the higher field [8, 9, 14–16]. However, the performance of the 3.0-T MR systems depends critically on a successful adaptation to the changed tissue relaxation times, to the increased absolute chemical shift difference between water and fat (in Hz), and to a potentially increased radiofrequency (RF) SAR [9]. These changes can cause poor image contrast, poor image resolution, or extended acquisition times if protocols optimized at 1.5 T are adapted directly for 3.0 T. Therefore a basic understanding and consideration of all factors which affect image quality is required to benefit efficiently from the high magnetic field strength.

Technical considerations

Signal, relaxation times, and tissue contrast

The SNR of MR images is influenced, among other things, by intrinsic tissue properties, the external magnetic field strength, and the pulse-sequence selection. The number of excitable spins per unit volume (proton density) and the tissue relaxation times (T1 and T2 relaxations times) are major determinants of MR signal intensity. A stronger magnetic field results in a larger longitudinal equilibrium magnetization. It also causes an increased precession frequency of the transverse magnetization. Both effects contribute to an MR signal increase at higher magnetic field strength that should dominate the increase in the detected noise. Thus the SNR is expected to linearly grow with the field strength in the field range of interest [17, 18]. This implies a doubled SNR at 3.0 T compared to 1.5 T. However, several other interfering factors need to be considered, such as the tissue relaxation times, number of acquired signals (NSA or NEX, number of excitations),

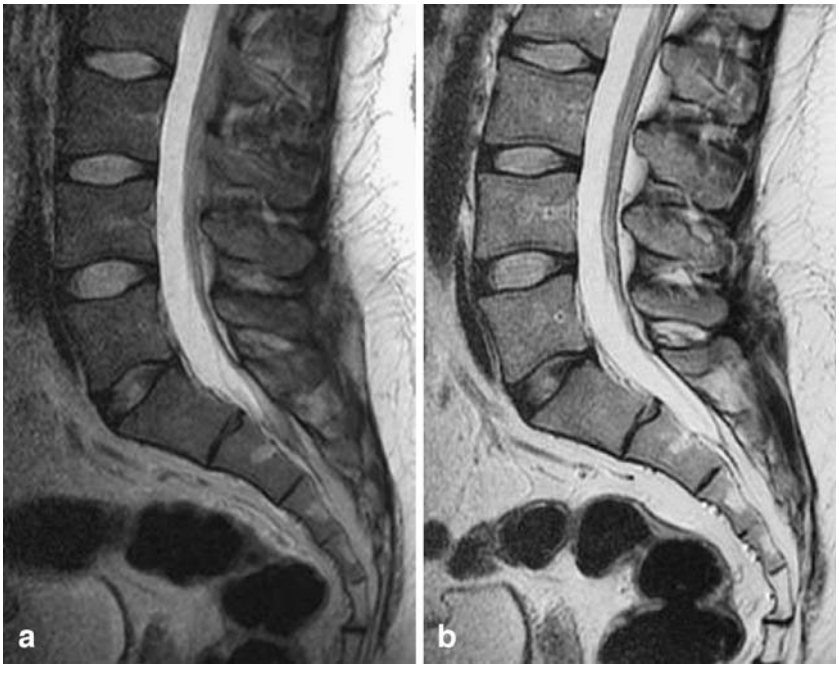

Fig. 1 Midsagittal T2-weighted FSE MR images from a 28-year-old patient with moderate low-back pain. **a**) At 3.0 T: TR 6238 ms, TE 120 ms, in-plane resolution 0.78×1.02 mm, field of view 240 mm, matrix 304×234, NSA 4; slice thickness 4 mm. **b**) At 1.5 T: TR 3000 ms, TE 111 ms, in-plane resolution 0.75×1.07 mm, field of view 240 mm, matrix 320×224, NSA 4, slice thickness 4 mm. On the image obtained at 3.0 T (**a**) the bone marrow signal intensity differs from that obtained at 1.5 T (**b**) due to the different T1 and T2 relaxation times

spatial resolution, receiver bandwidth, and choice and availability of optimized RF coils.

For several reasons an optimum balance between SNR and acquisition time may be even more difficult to achieve at higher field strengths and may require new solutions. One of the most important issues is the interaction between the magnetic field strength and the tissue relaxation times. It has been shown that T1 relaxation times are longer at 3.0 T than at 1.5 T [9, 17, 19, 20]. The T1 relaxation times of musculoskeletal tissues at 3.0 T were recently estimated to be 14–20% longer than those at 1.5 T [9]. In addition, the T1-lengthening effect of the field increase is more pronounced in fluid and fatty bone marrow and less pronounced in cartilage [9]. The T2 relaxation times depend less strongly on magnetic field strength. Several studies have shown a shortening of T2 values at 3.0 T by approx. 10% and by 10–20% at 4.0 T compared to 1.5 T [9]. All variations of the relaxation times have a direct impact on CNR and SNR (Fig. 1). For comparable repetition times (TR) optimized for 1.5 T imaging with spin-echo (SE) or fast spin-echo (FSE) sequences the contrast of T1-weighted images is lower at 3.0 T than at 1.5 T. Thus the longer T1 relaxation times imply longer TR to preserve high SNR and CNR (Fig. 2). Alternatively, inversion-recovery techniques may be used to restore the T1 contrast. Similarly, shorter echo times (TE) are needed to compensate the reduction of T2 and T2* relaxation times.

The attempt to preserve high SNR by a simple TR increase results in longer acquisition times in most cases. Prolonged examinations decrease patient tolerance, increase the risk of motion artifacts, decrease patient throughput, and directly affect the cost-effectiveness of an MR system [18]. In some cases the acquisition time may be kept short by a decrease in the number of acquisitions (NSA, NEX). A reduction by a factor of two doubles the examination speed at the cost of an SNR reduction by approx. 30%. In another straightforward attempt to shorten acquisition time the echo-train length (ETL) may be increased; however, longer echo trains can cause image blurring, particularly for short effective echo times (proton density and T1-weighted imaging with fast or turbo SE sequences), and increased motion artifacts and image distortions. A more promising option for keeping the scan times short while still observing high SNR and CNR is to exploit the synergy between the higher field strength and parallel imaging techniques.

Fig. 2 Midsagittal T2-weighted FSE MR image of the cervical and thoracic spine in 22-year-old healthy volunteer obtained at 3.0 T using a eight-channel spine coil. Imaging parameters: TR 4760 ms, TE 112.4 ms, in-plane resolution 0.81×0.88 mm, field of view 340 mm, matrix 416×384; NSA 4, slice thickness 3 mm, measuring time 4 min. High contrast between bone, intervertebral disc and CSF was obtained. (Images courtesy of Dr. Alfred Geissmann, Basel, Switzerland)

Chemical shift

The resonance frequency of a hydrogen nucleus at a given field strength depends on its chemical environment. Most hydrogen atoms in fat are bound to carbon atoms, and their nuclear magnetic moments have a lower resonance frequency than those of oxygen-bonded water hydrogen nuclei. Since the origin of MR signals is located in space on the basis of their resonance frequency in an applied magnetic field gradient, fat and water signals that originate from identical locations are mapped to different positions in the image [21]. This artifact, known as chemical shift artifact, is frequently seen in musculoskeletal imaging and can be clinically important in the evaluation of cartilage [10] or in the assessment of fluid containing structures surrounded by fat. In the latter case the transition zone between fluid and fat may simulate the presence of a pseudocapsule or significant changes in the wall thickness of fluid encapsulated lesions [22, 23]. The frequency difference between fat and water protons linearly increases with the magnetic field strength, from 74.5 Hz at 0.5 T, to147 Hz at 1.0 T, 224 Hz at 1.5 T, and to 448 Hz at 3.0 T. For identical receiver bandwidths the water vs. fat displacement in an image is therefore twice as large at 3.0 T than at 1.5 T. There are several options to address this.

The fat-water displacement in the image occurs along the frequency-encoding direction [21]. Thus one possibility is

to orient the chemical-shift displacement away from the anatomy of interest by exchanging the directions of the frequency- and phase-encoding gradients (Fig. 3). However, this may not be an option when artifacts associated with pulsatile flow that extend along the phase-encode direction are to be diverted from the anatomy of interest as well. For a constant number of image points in the frequency-encoding direction the magnitude of the fat-water displacement in pixels is inversely proportional to the receiver bandwidth of the pulse sequence. It can be reduced by an increase in bandwidth (Fig. 4). However, this causes a reduction in SNR, which typically scales with the inverse of the square root of the receiver bandwidth. When an identical fat-water shift is to be preserved upon a doubling of the field strength from 1.5 to 3.0 T, the receiver bandwidth must be doubled [24]. The SNR is then expected to increase by approx. 40% (square root of 2), since the SNR increase due to the higher field dominates the SNR loss caused by the increased receiver bandwidth. A higher bandwidth involves a faster sampling and allows a reduced minimum TE, which is favorable in the context of the shortened T2 times at the higher field strength. It also may allow a decreased acquisition time or an increase in the number of slices [24].

The increased absolute chemical-shift separation at 3.0 T may also be used to advantage. Firstly, it results in a better resolution of distinct resonances in MR spectroscopy and tends to cause spin systems to be less strongly coupled. Thus more metabolites and coupling patterns can be identified and quantification is facilitated. Secondly, the increased separation of fat and water signals measured in Hz (approx. 448 at 3.0 T vs. 215 Hz at 1.5 T) may facilitate and improve the fat saturation at 3.0 T, although this advantage may partly be offset by the increased resonance-frequency differences caused by susceptibility variations. In any case the increased chemical-shift separation allows a shortening of the fat-saturation pulses, with either frequency-selective or spectral-spatially selective pulses. Thus the overhead time spent with fat saturation during a multi-section acquisition at 3.0 T may be lower than at 1.5 T. Inversion-recovery based fat suppression techniques are also effective at 3.0 T; however, the inversion-recovery times need to be adapted.

Susceptibility

Every tissue or material placed in a strong magnetic field strength is magnetized and creates an additional local magnetic field component. The magnitude and the direction of the local field depend on the magnetic susceptibility, which is characteristic for the material placed in the field. Both air and various tissues and materials have different magnetic susceptibilities, which implies that the resonance-frequency of protons located in different areas in the body differ although magnet itself produces a homogeneous field. However, the basic process of image formation in MR imaging assumes the magnetic field strength to be the same everywhere as long as no gradients are applied. Thus protons with shifted resonance frequencies, due to variations in the local magnetic susceptibility, are imaged with a varying degree of susceptibility-induced displacement. This can result in object distortions, in hyperintense image regions with overlapping signals from neighboring regions, and in hypointense image regions. Additionally, in regions of steep local susceptibility changes, as in the vicinity of metallic materials or bone-tissue and air-tissue interfaces, the magnetic field experienced by protons in a single voxel can strongly vary. Then the transverse voxel magnetization rapidly decays, due to the widely spread Larmor frequencies. On the MR images this translates into very low signal intensity for most pulse sequences. The spatial misregistration and intravoxel dephasing can interfere with the

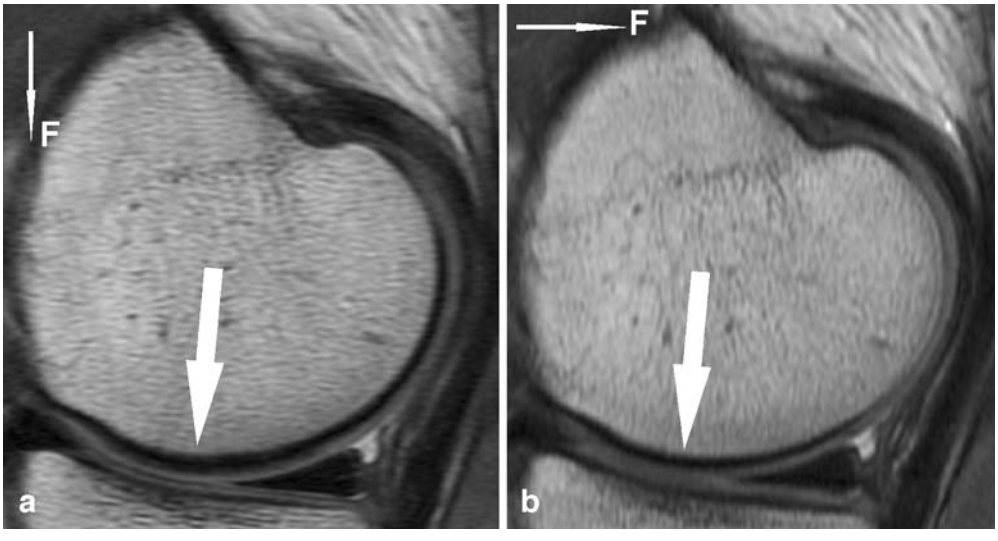

Fig. 3 Sagittal intermediate-weighted FSE MR images of the knee in a 24-year-old volunteer obtained at 3.0 T using the following imaging parameters: TR 1800 ms, TE 31.5 ms, in-plane resolution 0.29×0.67 mm, field of view 130 mm, matrix 448×192, receiver bandwidth 31.3 kHz, slice thickness 3 mm, NSA 4. The images were obtained first with frequency-encoding (*F*) in superior-inferior direction (**a**) and then in anterior-posterior directions (**b**). The artifactual thickening of the cortical bone due to chemical shift (*arrow*, **a**) decreases by exchanging the directions of the frequency- and phase-encoding gradients (**b**)

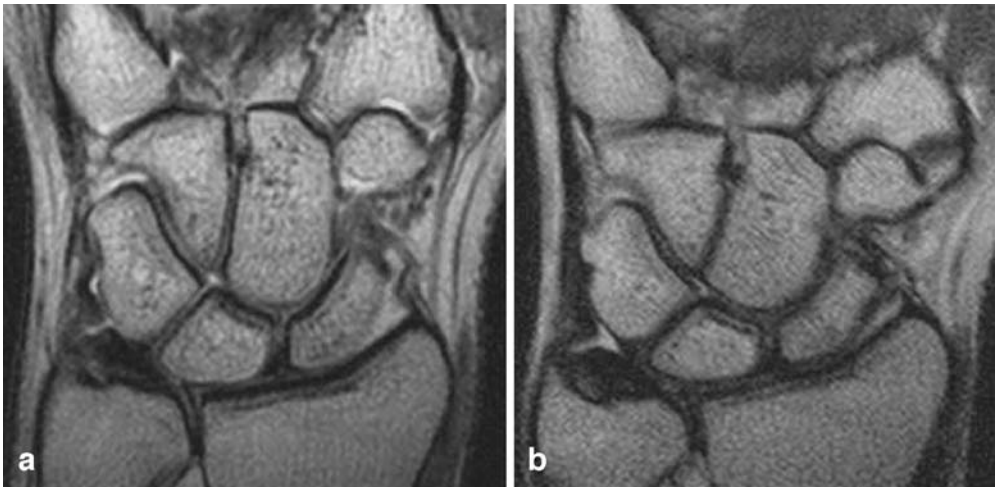

Fig. 4 SNR of bone and cartilage in intermediate-weighted FSE of the wrist at 3.0 T (**a**) and 1.5 T (**b**) in a 34-year-old volunteer. SNR of bone (410) and cartilage (124) is greater at 3.0 T than at 1.5 T (205 and 85, respectively). The images were obtained with a similar rectangular surface coil (note: this is not a dedicated wrist coil) at both field strengths. Imaging parameters: TR 1,800 ms, TE 17 ms, in-plane resolution 0.20×0.20 mm, field of view 100 mm, matrix 256×512, NSA 4; slice thickness 4 mm. An increased receiver bandwidth of 148 Hz/pixel was used at 3.0 T (**a**) than a 104.2 Hz/pixel at 1.5 T (**b**) to reduce the chemical shift artifacts

assessment of pathological or nonpathological conditions. Since the magnitude of susceptibility phenomena increases with the power of the field strength, the effects are considerably larger at 3.0 T than at 1.5 T. Pseudoenlargement of bones, "blooming" artifacts due to calcifications or chronic hemorrhage, and the severe signal loss caused by the metallic implants or ferromagnetic particles may lead to difficulty in assessing pathological conditions [25–27]. The fat signal suppression may be inhomogeneous in the presence of susceptibility-induced variations in the resonance frequencies. It fails principally near fat-air interfaces oriented perpendicularly to the main magnetic field and in the vicinity of metallic implants [21].

There are several possibilities to influence and/or reduce susceptibility-related effects. The direction of the frequency-encoding gradient may be changed, the voxel size may be minimized (small field-of-view and thin slices), or special devices may be used to replace the air from the vicinity of the region of interest [21, 28–31]. In addition, the shim process during the prescan may be optimized to homogenize the field strength in a restricted target volume of interest. Gradient-recalled echo (GRE) sequences are particularly sensitive to susceptibility artifacts because of the absence of the 180° refocusing pulse. Using the shortest echo times obtainable with increased receiver bandwidths can minimize the effects. Minimum TR times should be targeted with steady-state free precession (SSFP) based sequences. SE and FSE sequences are less affected but are associated with higher RF SAR especially when investigating a large volume of tissue (e.g., hip, spine).

Radiofrequency specific absorption rate

The RF SAR, measured in units of watts per kilogram body weight, represents the dosimetric value of the RF energy absorbed by the body tissues. A small part of the irradiated energy is absorbed by the body and transformed into heat, resulting in an increase in tissue temperature. For safety reasons the SAR values in clinical MR imaging are controlled by the scanner with the aim of avoiding raises in tissue temperature that exceed 1°C [32]. Although no significant biological risks for patients have yet been consistently confirmed [32, 33], the implications of the SAR for imaging at higher field strength is subject to reevaluation with the increased availability of systems at higher magnetic field. Among the factors which influence the SAR are tissue properties (e.g., conductivity) as well as the configuration of the MR system (e.g., the magnetic field strength, the pulse sequence, the coil used for radiofrequency irradiation) and the patient position in relation to the irradiating RF coil [33, 34]. The Larmor frequency linearly increases with the magnetic field strength and the irradiated power scales with the square of the Larmor frequency [35]. Therefore for identical pulse-sequence parameters a fourfold SAR increase associated with the doubling of the magnetic field strength may not be unrealistic. In addition, with the reduced wave length of the RF waves in the body at the higher field-strength inhomogeneous power absorption and the formation of so-called "hot spots" are of increased concern at higher field strength, in particular in the presence of metallic implants. Thus some scanners may have restricted the irradiated power to even lower limits at 3.0- than at 1.5 T, which may represent a limiting factor in the optimization of scan. SE and FSE pulse sequences are generally associated with

particularly high SAR values. Preparation pulses achieving magnetization transfer contrast (MTC) or fat saturation may significantly contribute to increased SAR levels for all pulse sequence types [8, 34]. For musculoskeletal imaging the SE and FSE sequences are of particular interest as they are most commonly employed. Although the prolongation of spin-echo scans due to SAR limits was a significant drawback in the initial studies comparing MR protocols at 3.0 T with similar protocols at 1.5 T, such as the study from Saupe et al. [8], technical solutions are now available for a better SAR management. For multiple SE sequences the "variable flip angle" and "hyper-echo" techniques have been developed which may reduce the absorbed RF power by a factor of 2.5–6 with no loss in signal intensity and only negligible changes in image contrast [36, 37]. Variable-flip-angle sequences, as all other sequences, can also be applied in combination with parallel imaging techniques to flexibly optimize the SAR in a trade-off with examination time and image quality [38].

Current status of musculoskeletal MR imaging at 3.0 T

MR imaging at 1.5 T has proven effective for almost all musculoskeletal applications. Some limitations concern the evaluation of the morphology of small intra-articular structures, such as ligaments, cartilage, and nerves and the detection of subtle pathological changes. New advances in therapeutic procedures and a few inconclusive correlations between clinical syndromes and imaging studies [39] have created the need for improved diagnostic performance, based primarily on a higher spatial resolution and a better tissue contrast (Fig. 4). Progress in this direction may now be possible with the recent introduction and increased availability of 3.0-T MR systems. Several authors have demonstrated that shorter acquisitions with higher SNR, CNR, and improved spatial resolution are possible at the higher magnetic field strength [8, 10, 16, 39–43].

SE, FSE, and GRE pulse sequences, with or without fat signal suppression, are currently the most frequently used sequences in routine musculoskeletal MR imaging. Saupe et al. [8] demonstrated that with identical receive coil geometries these sequences image the wrist with higher SNR and CNR at 3.0 T than at 1.5 T even when identical parameters optimized for 1.5 T are used. In T1-weighted SE images the SNR of muscle and bone at 3.0 T exceeded that at 1.5 T by a factor of 1.1 and 1.28, respectively. The CNR between bone and muscle and between bone and cartilage was also improved at 3.0 T. These results were obtained with the same imaging parameters, i.e., identical TR, TE, number of acquisitions, field of view, matrix size, and section thickness, and without increasing the examination time at 3.0 T. In images obtained with an intermediate-weighted FSE and a spoiled GRE sequence the SNR and CNR of cartilage, bone and muscle were 1.2–1.9, and 1.6–2.6 times higher than at 1.5 T, respectively. However, in this comparison, with all other parameters (including TR, TE, matrix size, and flip angle) being constant, the examination time was doubled at 3.0 T due to SAR limitations. The scan had to be split into the separate acquisition of two-slice stacks with a concomitant prolongation of the scan time. Qualitatively, the visibility of various small anatomical structures, such as the triangular fibrocartilage complex, intercarpal cartilage, median and ulnar nerves, was rated significantly higher on T1-weighted SE and intermediate-weighted FSE images obtained at 3.0 T than at 1.5 T. In summary, although the study by Saupe et al. [8] used a standard protocol optimized for imaging at 1.5 T at both field strengths, the results indicated advantages of 3.0 T, including higher SNR and tissue contrast and better visualization of various structures, with identical or slightly longer examination times (Fig. 5). Similar results have also been reported by other authors [44] who demonstrate improved image quality and higher wrist ligaments detection rates at 3.0 T than at 1.5 T. In the latter study [44] MR images with identical resolution (voxel size, image matrix, field of view) were acquired at both field strengths.

Masi et al. [16] compared the diagnostic performance of at 3.0- and at 1.5 T with regard to the detection of artificially induced cartilage lesions in knees using a porcine model. They compared fat-suppressed intermediate-weighted FSE sequences and three-dimensional GRE sequences, both with identical acquisition times at the two field strengths. They found improved subjective evaluation of image quality and increased SNR values at 3.0 T. The evaluation of the 3.0 T images detected the lesions with higher accuracy for the intermediate-weighted FSE sequence as well as the spoiled GRE sequence. These results [16] were confirmed by a study of Link et al. [15] who showed that with optimized high-resolution MR sequences the detection of cartilage lesions is better at 3.0 T than at 1.5 T.

Kornaat et al. [45] compared articular cartilage SNR, CNR, and thickness measurements on a 1.5-T and 3.0-T MR scanner using a three-dimensional spoiled GRE sequence and two three-dimensional SSFP sequences in knees of asymptomatic volunteers. They reported greater SNR and CNR efficiency at 3.0 T than at 1.5 T.

Although these studies show that MR imaging at 3.0 T may outperform imaging at 1.5 T or lower field strength with regard to SNR, CNR, and visualization of anatomical structures, many radiologists working with 3.0-T MR scanners have been initially disappointed by the image quality in daily clinical work. This may be due to various reasons. One important issue was the (non-)availability of dedicated surface coils for 3.0 T imaging. Dedicated surface coils optimized for imaging of specific anatomical regions play an important role in improving both SNR and spatial resolution (Fig. 6). However, until now, such coils are not generally available for MR imaging at 3.0 T. A 10% lower signal intensity and a more inhomogeneous magnetic

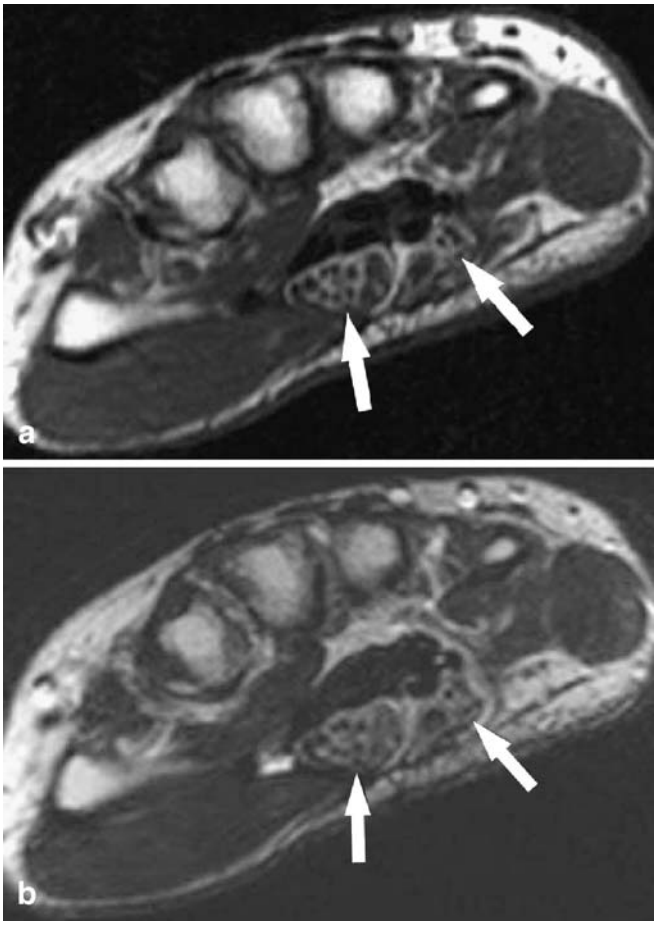

Fig. 5 Transverse SE-weighted MR images from a 55-year-old patient with suspected carpal mass obtained at 3.0 T (**a**) and 1.5 T (**b**). A simultaneous fibrolipohamartoma of the median and ulnar nerves is seen on both images (*arrows*). The internal structure and the extension of tumor is significantly better assessed on the image obtained at 3.0 T (**a**). The images were obtained with a similar rectangular surface coil using same imaging parameters: TR 500 ms, TE 20 ms, in-plane resolution 0.20×0.20 mm, field of view 100 mm, matrix 256×512, NSA 4; slice thickness 4 mm

field were found at 3.0 T than at 1.5 T for imaging with similar pulse sequences and a standard head coil [46]. Preliminary work by Bauer et al. [47] has shown up to threefold greater in SNR that with an optimized coil design at 3.0 T vs. standard 1.5 T imaging. Similarly, De Zanche et al. [48] demonstrated excellent signal uniformity and SNR for MR imaging of the wrist at 3.0 T with a dedicated receive-coil array. In their preliminary work they showed that their tightly arranged, preamplifier-decoupled small coils provide an in-plane resolution of 390×390 μm in 30 s of GRE imaging. Using parallel imaging the SNR advantage of such coils can be flexibly traded for scan speed. Another important condition for the success of 3.0 T MR systems is the availability of optimized sequences. In the early stage of clinical 3.0 T imaging the use of SE and FSE sequences, which are still the workhorses in musculoskeletal MR imaging, was often limited by SAR constraints. However, with the advent of the variable-flip-angle sequences [36, 37, 49] the situation has significantly improved.

The latest generation of 3.0-T MR scanners now offers optimized coils as well as optimized sequences for musculoskeletal imaging. Although experience is still limited, it seems likely that with these systems the potential benefits of the higher field can be better realized in clinical practice than was possible even 1 year ago.

For musculoskeletal conditions (i.e., degenerative spine disorders, tendon lesions, soft tissue tumors, and bone marrow disorders) the image quality of current imaging protocols at 1.5 T results in adequate diagnostic performance. In these cases the expected improvement in the introduction of 3.0 T will probably consist mainly in a shortening of the examination times and a higher patient throughput (Fig. 7).

The higher magnetic field strength also needs to be considered in MR arthrography. It is known that iodinated contrast agents, which facilitate the intra-articular needle placement, reduce the gain in MR signal intensity obtained from gadolinium-based contrast agents [46, 50]. These effects are reported to be stronger at 3.0 T, which suggests a careful minimization of the volume of iodinated agent at 3.0 T [46]. The generally higher MR signal intensity at 3.0 T also pertains to fluids containing one of the gadolinium-based contrast agents used in arthrography. Masi et al. [46] have shown in a phantom study with typical T1- and intermediate-weighted sequences at 3.0 T that the maximum signal is observed at slightly lower contrast-agent concentration than at 1.5 T. Since the image contrast vs. native intra- and extra-articular tissues may be improved due to the longer native T1 relaxation times, the optimum contrast-agent concentration may be somewhat lower at 3.0- than at 1.5 T. However, further in vivo studies are necessary to investigate the relationship between CNR and the contrast-agent concentration at 3.0 T.

Future perspectives of musculoskeletal imaging at 3.0 T

Several studies have shown a potential of 3.0 T MR imaging in assessing pathology of the cartilage surface when using intermediate-weighted FSE sequences or spoiled GRE sequences. SSFP-based (e.g., trueFISP, DESS, CISS, FIESTA) sequences are under evaluation for cartilage assessment. They provide high-resolution three-dimensional data sets with an image contrast that depends on the ratio of T2 to T1 [43]. T2 mapping of the cartilage is a functional quantitative technique based on different MR pulse-sequence types, including FSE and echo-planar imaging, which may allow conclusions on spatially localized variations in the water content of cartilage [51]. Areas of increased or decreased water content are correlated with cartilage damage. The increased

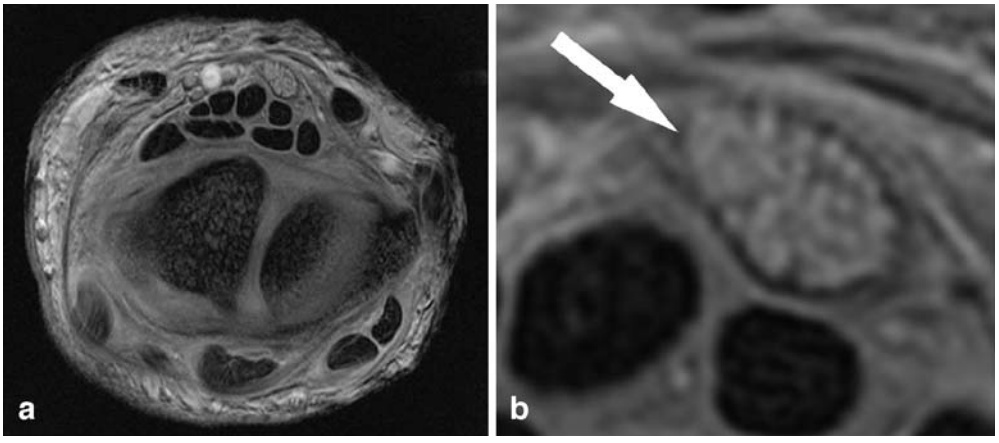

Fig. 6 Transverse high-resolution two-dimensional GRE-weighted MR image of the wrist obtained at 3.0 T in a 40-years-old volunteer using a dedicated six-element array coil. Imaging parameters: TR 16.8 ms, TE 6.9 ms, in-plane resolution 182×228 μm, field of view 70 mm, matrix 384×310, NSA 4. The coil system and the parallel imaging performance enables a high SNR and image uniformity in a short acquisition time (160 s). The high in-plane resolution permits a good visualization of fascicles within the median nerve. (Images courtesy of Dr. Nicola de Zanche, University and ETH, Zurich, Switzerland)

SNR obtained at 3.0 T should improve the accuracy of such measurements, but further studies are needed.

Several authors have demonstrated that the perineurium and the individual internal fascicles can be accurately assessed at 3.0 T [39, 40]. Evaluation of peripheral nerves at higher magnetic field strength (Fig. 6) may be important in surgical repairs after injuries, for the differentiation of inflammatory and degenerative changes, and for the identification of the exact origin of tumors (i.e., perineural or intraneural) [40, 52].

Fig. 7 Coronal fat-suppressed intermediate-weighted FSE MR images from a 37-year-old patient at 3.0 T in a measuring time of 1 min and 25 s using a four-channel knee coil. An increased signal intensity in soft tissues between iliotibial band and lateral femoral condyle (*arrow*) is identified in this patient, consistent with iliotibial friction syndrome after sustained running activity. Parameters: TR 2480 ms, TE 33.4 ms, in-plane resolution 0.4×0.8 mm, field of view 130 mm, matrix 320×160, NSA 2; slice thickness 4 mm. Note the excellent fat saturation throughout the image. (Images courtesy of Dr. Alfred Geissmann, Basel, Switzerland)

Spectroscopy is another area of MR imaging which will be fostered by the use of 3-T MR imaging. Pfirrmann et al. [53] recently reported the use of single-voxel proton spectroscopy for the evaluation of fat content in the supraspinatus muscle of asymptomatic volunteers and patients with supraspinatus lesions using a 1.5-T MR scanner. Preliminary data from Wang et al. [54] show that ^{1}H-spectroscopy may be helpful in differentiating between benign and malignant musculoskeletal tumors.

The skillful application of parallel imaging techniques is another area which may boost the performance of 3.0-T scanners. Although parallel imaging techniques are not yet an integral part of musculoskeletal MR imaging protocols in most institutions, preliminary experience suggests that they may be valuable for a fast imaging of internal traumatic derangements of the hip, knee, and ankle [55]. High field imaging and parallel imaging complement each other in potent synergy combined [56]. Parallel imaging offers the opportunity of converting the additional SNR at high fields into a variety of other benefits such as speed, resolution, artifact suppression, SAR reduction, and mitigation of acoustic noise caused by gradient switching and thus provides a formidably increased flexibility in the optimization of scan protocols.

Conclusion

The introduction of 3.0-T whole-body MR systems has further increased the interest in imaging the musculoskeletal system. The increased MR signal available at higher magnetic fields can flexibly be traded for spatial-resolution increase and acquisition-time reduction. An optimization of pulse sequences, pulse-sequence parameters, and RF

coils, which considers the changes in T1 and T2 relaxation times SAR, chemical shift, and susceptibility is important when switching from 1.5 to 3.0 T. Although it is difficult to predict whether 3.0 T systems will represent the new standard for examinations of the musculoskeletal system, recent technical advances in coil technology and pulse-sequence design suggest that MR imaging at 3.0 T will consolidate its role as an important diagnostic tool for disorders of the musculoskeletal system.

References

1. Livstone BJ, Parker L, Levin DC (2002) Trends in the utilization of MR angiography and body MR imaging in the US Medicare population: 1993–1998. Radiology 222:615–618
2. Savnik A, Malmskov H, Thomsen HS et al (2001) MRI of the arthritic small joints: comparison of extremity MRI (0.2 T) vs high-field MRI (1.5 T). Eur Radiol 11:1030–1038
3. Taouli B, Zaim S, Peterfy CG et al (2004) Rheumatoid arthritis of the hand and wrist: comparison of three imaging techniques. Am J Roentgenol 182:937–943
4. Morakkabati-Spitz N, Gieseke J, Kuhl C et al (2005) MRI of the pelvis at 3 T: very high spatial resolution with sensitivity encoding and flip-angle sweep technique in clinically acceptable scan time. Eur Radiol 1–8
5. Morakkabati-Spitz N, Gieseke J, Kuhl C et al (2005) 3.0-T high-field magnetic resonance imaging of the female pelvis: preliminary experiences. Eur Radiol 15:639–644
6. Gutberlet M, Schwinge K, Freyhardt P et al (2005) Influence of high magnetic field strengths and parallel acquisition strategies on image quality in cardiac 2D CINE magnetic resonance imaging: comparison of 1.5 T vs. 3.0 T. Eur Radiol 15:1586–1597
7. Lutterbey G, Gieseke J, von Falkenhausen M, Morakkabati N, Schild H. Lung (2005) MRI at 3.0 T: a comparison of helical CT and high-field MRI in the detection of diffuse lung disease. Eur Radiol 15:324–328
8. Saupe N, Prussmann KP, Luechinger R, Bosiger P, Marincek B, Weishaupt D (2005) MR imaging of the wrist: comparison between 1.5- and 3-T MR imaging-preliminary experience. Radiology 234:256–264
9. Gold GE, Han E, Stainsby J, Wright G, Brittain J, Beaulieu C (2004) Musculoskeletal MRI at 3.0 T: relaxation times and image contrast. Am J Roentgenol 183:343–351
10. Gold GE, Suh B, Sawyer-Glover A, Beaulieu C (2004) Musculoskeletal MRI at 3.0 T: initial clinical experience. Am J Roentgenol 183:1479–1486
11. Gold GE, Reeder SB, Beaulieu CF (2004) Advanced MR imaging of the shoulder: dedicated cartilage techniques. Magn Reson Imaging Clin N Am 12:143–159, vii
12. Collins CM, Smith MB (2001) Signal-to-noise ratio and absorbed power as functions of main magnetic field strength, and definition of "90 degrees" RF pulse for the head in the birdcage coil. Magn Reson Med 45:684–691
13. Sommer T, Hackenbroch M, Hofer U et al (2005) Coronary MR angiography at 3.0 T versus that at 1.5 T: initial results in patients suspected of having coronary artery disease. Radiology 234:718–725
14. Farooki S, Ashman CJ, Yu JS, Abduljalil A, Chakeres D (2002) In vivo high-resolution MR imaging of the carpal tunnel at 8.0 tesla. Skelet Radiol 31:445–450
15. Link TM, Sell CA, Masi JN et al (2005) 3.0 vs 1.5 T MRI in the detection of focal cartilage pathology-ROC analysis in an experimental model. Osteoarthr Cartil 14:63–70
16. Masi JN, Sell CA, Phan C et al (2005) Cartilage MR imaging at 3.0 versus that at 1.5 T: preliminary results in a porcine model. Radiology 236:140–150
17. Maubon AJ, Ferru JM, Berger V et al (1999) Effect of field strength on MR images: comparison of the same subject at 0.5:1.0, and 1.5 T. Radiographics 19:1057–1067
18. Mitchell D, Cohen M (2004) MRI principles. Saunders, Philadelphia
19. Duewell SH, Ceckler TL, Ong K et al (1995) Musculoskeletal MR imaging at 4 T and at 1.5 T: comparison of relaxation times and image contrast. Radiology 196:551–555
20. Kangarlu A, Abduljalil AM, Robitaille PM (1999) T1- and T2-weighted imaging at 8 Tesla. J Comput Assist Tomogr 23:875–878
21. Peh WC, Chan JH (2001) Artifacts in musculoskeletal magnetic resonance imaging: identification and correction. Skelet Radiol 30:179–191
22. Dwyer AJ, Knop RH, Hoult DI (1985) Frequency shift artifacts in MR imaging. J Comput Assist Tomogr 9:16–18
23. Whitehouse RW, Hutchinson CE, Laitt R, Jenkins JP, Jackson A (1997) The influence of chemical shift artifact on magnetic resonance imaging of the ligamentum flavum at 0.5 tesla. Spine 22:200–202
24. Schick F (2005) Whole-body MRI at high field: technical limits and clinical potential. Eur Radiol 15:946–959
25. Tien RD, Buxton RB, Schwaighofer BW, Chu PK (1991) Quantitation of structural distortion of the cervical neural foramina in gradient-echo MR imaging. J Magn Reson Imaging 1:683–687
26. Heindel W, Friedmann G, Bunke J, Thomas B, Firsching R, Ernestus RI (1986) Artifacts in MR imaging after surgical intervention. J Comput Assist Tomogr 10:596–599
27. Allkemper T, Schwindt W, Maintz D, Heindel W, Tombach B (2004) Sensitivity of T2-weighted FSE sequences towards physiological iron depositions in normal brains at 1.5 and 3.0 T. Eur Radiol 14:1000–1004
28. Cox H, Dillon WP (1995) Low-cost device for avoiding bulk susceptibility artifacts in chemical-selective fat saturation MR of the head and neck. Am J Neuroradiol 16:1367–1369
29. Taber KH, Herrick RC, Weathers SW, Kumar AJ, Schomer DF, Hayman LA (1998) Pitfalls and artifacts encountered in clinical MR imaging of the spine. Radiographics 18:1499–1521
30. Eustace S, Jara H, Goldberg R et al (1998) A comparison of conventional spin-echo and turbo spin-echo imaging of soft tissues adjacent to orthopedic hardware. Am J Roentgenol 170:455–458
31. Suh JS, Jeong EK, Shin KH et al (1998) Minimizing artifacts caused by metallic implants at MR imaging: experimental and clinical studies. Am J Roentgenol 171:1207–1213

32. Price RR (1999) The AAPM/RSNA physics tutorial for residents. MR imaging safety considerations. Radiological Society of North America. Radiographics 19:1641–1651
33. Shellock FG, Crues JV (2004) MR procedures: biologic effects, safety, and patient care. Radiology 232:635–652
34. Shellock FG (2000) Radiofrequency energy-induced heating during MR procedures: a review. J Magn Reson Imaging 12:30–36
35. Lin C, Bernstein MA, Gibbs GF, Huston J 3rd (2003) Reduction of RF power for magnetization transfer with optimized application of RF pulses in k-space. Magn Reson Med 50:114–121
36. Hennig J, Weigel M, Scheffler K (2003) Multiecho sequences with variable refocusing flip angles: optimization of signal behavior using smooth transitions between pseudo steady states (TRAPS). Magn Reson Med 49:527–535
37. Busse RF (2004) Reduced RF power without blurring: correcting for modulation of refocusing flip angle in FSE sequences. Magn Reson Med 51:1031–1037
38. Pruessmann KP, Weiger M, Scheidegger MB, Boesiger P (1999) SENSE: sensitivity encoding for fast MRI. Magn Reson Med 42:952–962
39. Monagle K, Dai G, Chu A, Burnham RS, Snyder RE (1999) Quantitative MR imaging of carpal tunnel syndrome. Am J Roentgenol 172:1581–1586
40. Ikeda K, Haughton VM, Ho KC, Nowicki BH (1996) Correlative MR-anatomic study of the median nerve. Am J Roentgenol 167:1233–1236
41. Lazovic-Stojkovic J, Mosher TJ, Smith HE, Yang QX, Dardzinski BJ, Smith MB (2004) Interphalangeal joint cartilage: high-spatial-resolution in vivo MR T2 mapping-a feasibility study. Radiology 233:292–296
42. Mosher TJ, Smith HE, Collins C et al (2005) Change in knee cartilage T2 at MR imaging after running: a feasibility study. Radiology 234:245–249
43. Gold GE, McCauley TR, Gray ML, Disler DG (2003) What's new in cartilage? Radiographics 23:1227–1242
44. Lenk S, Ludescher B, Martirosan P, Schick F, Claussen CD, Schlemmer HP (2004) 3.0 T high-resolution MR imaging of carpal ligaments and TFCC. Rofo Fortschr Geb Rontgenstr Neuen Bildgeb Verfahr 176:664–667
45. Kornaat PR, Reeder SB, Koo S et al (2005) MR imaging of articular cartilage at 1.5 T and 3.0 T: comparison of SPGR and SSFP sequences. Osteoarthr Cartil 13:338–344
46. Masi JN, Newitt D, Sell CA et al (2005) Optimization of gadodiamide concentration for MR arthrography at 3 T. Am J Roentgenol 184:1754–1761
47. Bauer J, Rosss C, Li X, Carballiodo-Gamio J, Banerjee S, Krug R (2005) Optimization and reproducibility evaluation of volumetric cartilage measurements of the knee and 1.5 T and 3 T. In: Proceeding of the ISMRM, Miami
48. De Zanche N, Leussler C, Mandelkow H, Pruessman KP (2005) A 6-element array for parallel wrist imaging at 3 tesla. In: Proceeding of the ISMRM, Miami
49. Hennig J, Scheffler K (2001) Hyperechoes. Magn Reson Med 46:6–12
50. Montgomery DD, Morrison WB, Schweitzer ME, Weishaupt D, Dougherty L (2002) Effects of iodinated contrast and field strength on gadolinium enhancement: implications for direct MR arthrography. J Magn Reson Imaging 15:334–343
51. Gold GE, Thedens DR, Pauly JM et al (1998) MR imaging of articular cartilage of the knee: new methods using ultrashort TEs. Am J Roentgenol 170:1223–1226
52. Heddings A, Bilgen M, Nudo R, Toby B, McIff T, Brooks W (2004) High-resolution magnetic resonance imaging of the human median nerve. Neurorehabil Neural Repair 18:80–87
53. Pfirrmann CW, Schmid MR, Zanetti M, Jost B, Gerber C, Hodler J (2004) Assessment of fat content in supraspinatus muscle with proton MR spectroscopy in asymptomatic volunteers and patients with supraspinatus tendon lesions. Radiology 232:709–715
54. Wang CK, Li CW, Hsieh TJ, Chien SH, Liu GC, Tsai KB (2004) Characterization of bone and soft-tissue tumors with in vivo 1H MR spectroscopy: initial results. Radiology 232:599–605
55. Romaneehsen B, Oberholzer K, Muller LP, Kreitner KF (2003) Rapid musculoskeletal magnetic resonance imaging using integrated parallel acquisition techniques (IPAT)-initial experiences. Rofo Fortschr Geb Rontgenstr Neuen Bildgeb Verfahr 175:1193–1197
56. Pruessmann KP (2004) Parallel imaging at high field strength: synergies and joint potential. Top Magn Reson Imaging 15:237–244